Scientific paper

Structural, Morphological and Electrical Properties of $La_{1-x}Sr_xAlO_{3-\delta}$ (x = 0, 0.1, 0.15) Synthesized by the Pechini Method

Farida Bouremmad,[1,*] Abderrahim Benabbas,[1] Hachemi Bouridah,[2] Kamel Rida,[1] Shalima Shawuti[3] and Mehmed Ali Gülgün[3]

[1] *Laboratoire de l'Interaction des Matériaux et de l'Environnement L.I.M.E., Université de Jijel, 18000 Jijel, Algérie.*

[2] *Laboratoire d'Etude des Matériaux L.E.M, Université de Jijel, 18000 Jijel, Algérie.*

[3] *Sabanci University, FENS, Orhanli Tuzla, Istanbul 34956 Turkey*

** Corresponding author: E-mail: bouremmad_farida@yahoo.com*

Received: 15-05-2012

Abstract

$La_{1-x}Sr_xAlO_{3-\delta}$ (x = 0, 0.1, 0.15) fine particles were prepared by the Pechini process using citric acid and ethylene glycol at low temperature 900 °C. The powders were studied by several physical characterization techniques. The FTIR spectrum of the resin treated at 200 °C revealed the formation of a metalorganic complex and a polymerized form of ethylene glycol. XRD spectra of the samples, calcined at 900 °C, illustrated a single phase $LaAlO_3$. However, $La_{0.9}Sr_{0.1}AlO_{3-\delta}$ and $La_{0.85}Sr_{0.15}AlO_{3-\delta}$ powders mainly consist of a deficient hexagonal perovskite phase with a small amount of a second phase ($LaSrAl_3O_7$). Ionic conductivities of these materials were studied by impedance spectroscopy in the range of 100–700 °C in air.

Keywords: Ionic conductivity, sol gel, solid oxide fuel cell, impedance spectroscopy, perovskite

1. Introduction

Materials with a high ionic conductivity can be obtained by introducing oxygen ion vacancies into a perovskite type oxide. Such aliovalent ion doped ceramics are currently of considerable interest primarily because of their possible application as solid electrolytes in solid oxide fuel cells. They also cater to a wide variety of other applications as catalysts for oxidation reaction and as oxygen sensors.[1–2]

$LaAlO_3$ type perovskite is a potential candidate for a cost effective solid electrolyte. The pure phase presents a very low ionic conductivity. An addition of divalent cations is expected to enhance the oxygen ion conduction.[3]

Earlier studies have shown that substitution of divalent cations in $LaAlO_3$ on the La site could raise the conductivity value. Most commonly, these phases were prepared by the classical solid state reaction method which requires repeated cycles of high temperatures in the range of 1500 °C–1700 °C and grinding.[4–5]

In contrast, soft solution techniques offer the possibility to work at low temperature (T ≤ ~1000 °C). Such routes facilitate homogenization of ions in solution. Soft chemical methods have shown their versatility in several oxide systems for preparing well-characterized mixed-oxide powders.[6–7] Among these methods we utilized the Pechini process in which, citric acid was used to chelate metal ions and ethyleneglycol was used as the solvent. Ethylene glycol also facilitates polymerization of the citric acid to form a metal-loaded resin. This resin inhibits metal ion segregation and achieves a homogeneous precursor for the mixed oxide.[8–9] For the pure $LaAlO_3$, the Pechini method was used by Popovichi et al,[10] where they discussed the synthesis and the crystalline structure.

This study is focused on the preparation of $La_{1-x}Sr_xAlO_{3-\delta}$ (x = 0, 0.1 and 0.15) by the Pechini process. Crystallinity and morphology were studied by FTIR, XRD and SEM. Ionic conductivity was determined by impedance analysis.

2. Experimental

The starting materials $La(NO_3)_2$ $6H_2O$, $Al(NO_3)_3$ $9H_2O$ and $Sr(NO_3)_2$ $4H_2O$ were dissolved in aqueous citric acid (CA) solution and ethylene glycol (EG) according to the molar ratio of (inorganic atoms):CA:EG = 1:10:40, the amount of the citric acid is 10 times more than that of the metal in order to avoid the precipitation of the metals salts which leads to a nonuniformity in the chelation metals. Then, the solution was heated at 90 °C while stirring until a clear gel was obtained. Increasing the temperature to 130 °C resulted in a spongy dark gel. No sign of precipitation was observed. This gel was further heated at 200 °C for 5 h and at 500 °C for 5 h to remove the solvents and the organic matter. The crisp precursor was then reground and calcined at 900 °C. Several techniques were employed to investigate the phases that formed at different stages of processing. FTIR spectroscopy measurements were carried out with a SHIMADZU FTIR 84005 apparatus for the gel and the calcined samples. FTIR spectra were scanned between 4000 and 400 cm^{-1}. The X-ray diffraction (XRD) experiments were performed on a D8 Advance Bruker AXS diffractometer with CuKα radiation equipped with a curved graphite monochromator. The data were collected in the 2θ range of 10–80° with a step size of 0.03° and a count time of 2 s per step. Scanning Electron Microscopy (SEM) images were recorded at room temperature on a LEO Supra 35VP FEG SEM (by ZEISS, Germany) apparatus. For the complex plane impedance, measurements were performed via a Solartron 1260 impedance analyzer with dielectric interface. The measurements were done in the temperature range between 100 °C–700 °C and the frequency range from 5Hz to 20MHz with a frequency step of 5 points per decade and an oscillating voltage of 100 mV. For high temperature measurements, a ProboStat setup was utilized.

3. Results and Discussion

The polymerized metalorganic complex as a complex-oxide precursor has proven to be an effective approach to reduce the processing temperatures, costs and times.[7] Using a polymerized complex route first introduced by M Pechini,[11] we followed different stages of processing of pure and Sr-doped $LaAlO_3$ powders for ionic conductor electrolytes.

3. 1. Precursor to Oxide Transformation

The complexation of the metal ion with the chelating carboxyl group was followed via Fourier transformed infrared (FTIR) spectroscopy. The FTIR spectra of the samples treated at different temperatures for 5h are illustrated in Figure 1. The results corresponding to $LaAlO_3$ processing are presented here. For the other two Sr-doped samples, the shape of the spectra and the trends in the behavior were very similar. FTIR spectra of the gel heated at 200 °C showed a broad band between 3600–3200 cm^{-1} characteristic of hydroxyl-groups.[12] Three bands related to carboxylate stretching modes were observed at 1736, 1635 and 1400 cm^{-1}.[13–14] The band at 1736 cm^{-1} could be assigned to the C=O stretching mode of the ester which was formed by polyesterification reaction of CA and EG. The original solution was rich in acid (CA) when compared to the cations. The 1635 cm^{-1} band could be assigned to the asymmetric COO- stretching mode for a unidentate complex, formed from the chelation of carboxyl group of CA and metal ions. The 1400 cm^{-1} band could be assigned to the symmetric COO– stretching mode from the chelation of the carboxyl group of CA and metal ions. The bands of 1635 and 1400 cm^{-1}, with $\Delta\nu = 235$ cm^{-1}, suggest that the gels contain one unidentate group in the structure.[15–16] The band at 1177 cm^{-1} is attributed to the C–C–O structure of ethylene glycol in the polymerization process.[17–19] With increasing the temperature to 500 °C, the FTIR spectrum showed significant changes (Figure 1). The band at 1487 cm^{-1} was due to the stretching vibration of CO_3^{2-} group. This indicated that carbonate salts formed and persisted until this temperature in the powder. The existence of NO^{3-} was revealed by the band located at 800 cm^{-1}.[20] For the sample heat treated at 900 °C, it can be noted that all bands corresponding to the organic phases and nitrates have disappeared. We also note that two bands at 667 cm^{-1} and 490 cm^{-1} persisted. They can be assigned to the metal oxide group (possibly, La–O and Al–O stretching frequencies).[21]

The XRD spectra of $La_{1-x}Sr_xAlO_{3-\delta}$ for x = 0.0 to 0.15, heated at 900 °C are plotted in Figure 2. Diffraction peaks arising from the perovskite phase were found in all samples illustrating that it was the major phase that formed. Peaks in the spectra were indexed according to the

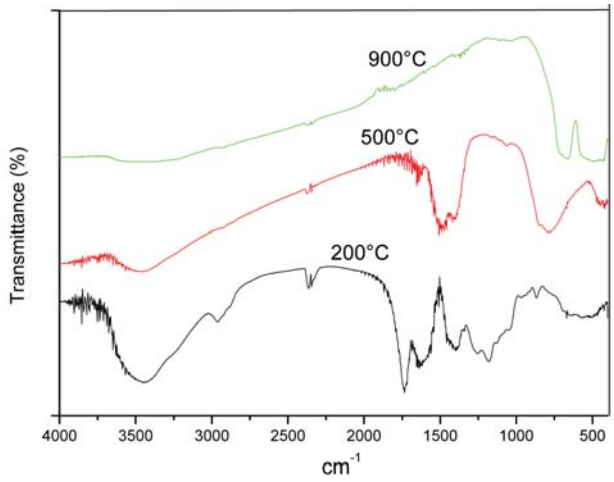

Fig. 1. FTIR spectra of the precursor gel for $LaAlO_3$ heat treated at different temperatures

hexagonal $LaAlO_3$ perovskite phase, with the lattice parameters of $a = 5.36301$ Å and $c = 13.12887$ Å (JCPDS card n° 09–0072). Figure 2 also illustrates that a single-phase perovskite was obtained for $LaAlO_3$ chemistry. However, for $La_{0.9}Sr_{0.1}AlO_{3-\delta}$ and $La_{0.85}Sr_{0.15}AlO_{3-\delta}$, additional peaks were found. These extra peaks could be assigned to a second phase indexed as $LaSrAl_3O_7$ (JCPDS card n° 50–1815).

The lattice parameters and the cell volume for perovskite phases were refined by using CELREF software in 2θ range of 10–80° and they are shown in Table I. Typically, two competing factors act on the variation of the lattice parameters: first, the substitution of La^{3+} by Sr^{2+}, which increases the volume, on the other hand, the creation of oxygen vacancies which acts in the opposite direction. From Table I, with an increase of Sr content from x = 0 to x = 0.1, the unit cell volume increased. This slight increase in the unit cell volume (~0.3%) could be due to both of the substitution of La^{3+} ions by Sr^{2+} ions and the difference between their ionic radii (La^{3+} = 1.36 Å, Sr^{2+} = 1.44 Å), thus we can say that the factor related to the substitution has dominated. However, the increase in the unit cell volume was limited to 0.2% when Sr doping amount was x = 0.15, in this case, the factor related to the creation of oxygen vacancies is dominating.

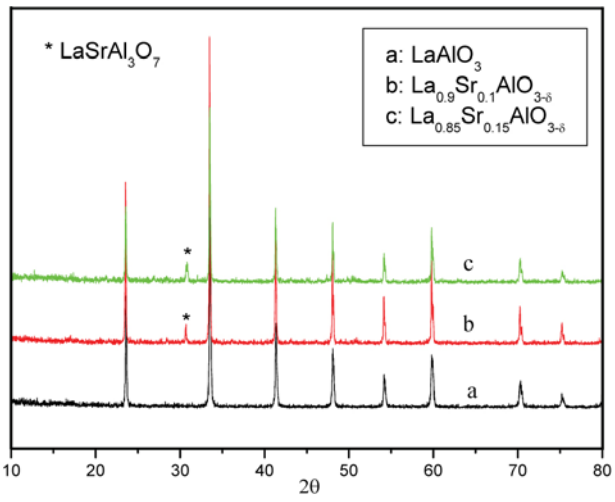

Fig. 2. XRD spectra of $La_{1-x}Sr_xAlO_{3-\delta}$ (x = 0; 0.1; 0.15) calcined at 900 °C.

Table 1. Cell parameters of $La_{1-x}Sr_xAlO_{3-\delta}$ (x = 0; 0.1; 0.15)

	a (Å)	*c (Å)*	V (Å^3)
$LaAlO_3$	5.3407	13.1193	324.067
$La_{0.9}Sr_{0.1}AlO_{3-6}$	5.3494	13.1195	325.128
$La_{0.85}Sr_{0.15}AlO_{3-6}$	5.3474	13.1160	324.799

The SEM microstructures of the samples are shown in Figure 3. The images show that the samples were constituted by aggregation of small particles. The size distribution of aggregates is also shown in Figure 4. The average size of the grains was determined by two methods:

- Using Scherrer's formula:

$$d = \frac{0.9\lambda}{\beta.\cos\theta} \quad (1)$$

Where d is the average crystallite size, λ is the wavelength of CuKα, β is the full width at half maximum intensity and θ is the Bragg's angle;

- Using a computer image processing technique (active contours image-processing method).[22]

The values for grain/crystallite sizes are shown in Table 2. Increasing the Sr contents leads to an increase in grain/crystallite size.

For $La_{0.85}Sr_{0.15}AlO_{3-\delta}$, results calculated with the help of Scherrer's formula and the image analysis method deviate strongly from each other (93 nm vs 600 nm). In the image analysis method, the measured value 600 nm was the size of the primary particles. This deviation is an indication that for the powders with x = 0.15 each primary particle may contain more than one crystallite. It must be also remembered that for samples with a large variation of crystallite sizes Scherrer's formula skews the results in favour of smaller crystal sizes that are in significant fractions.

For $LaAlO_3$ powders, the crystallite size found in this investigation is very similar to the values reported in the literature. Carazeanu Popovici,[10] reported 50 nm particle size for the $LaAlO_3$ powders. Chandradas et al,[23] prepared their $LaAlO_3$ powders by emulsion combustion method and determined a grain size of 60 nm.

Table 2. Grain/crystallite sizes

	Scherrer's formula (nm)	**Image treatment (nm)**
$LaAlO_3$	46	33
$La_{0.9}Sr_{0.1}AlO_{3-\delta}$	102	162
$La_{0.85}Sr_{0.15}AlO_{3-\delta}$	93	600

3. 2. Electrical Properties

Impedance spectroscopy is a technique for the characterization of the complex electrical behaviour of electrolytes. Total impedance of an ionic conductor contains contributions from bulk, grain-boundaries and electrode-electrolyte interfaces at high, middle and low frequencies.[24] Impedance spectra are best represented in a Nyquist plot form, where the imaginary part Z" is plotted against the real part Z'. Usually, for different phenomena cited above, three successive arcs are observed in the Nyquist representation associated with an RC model-cir-

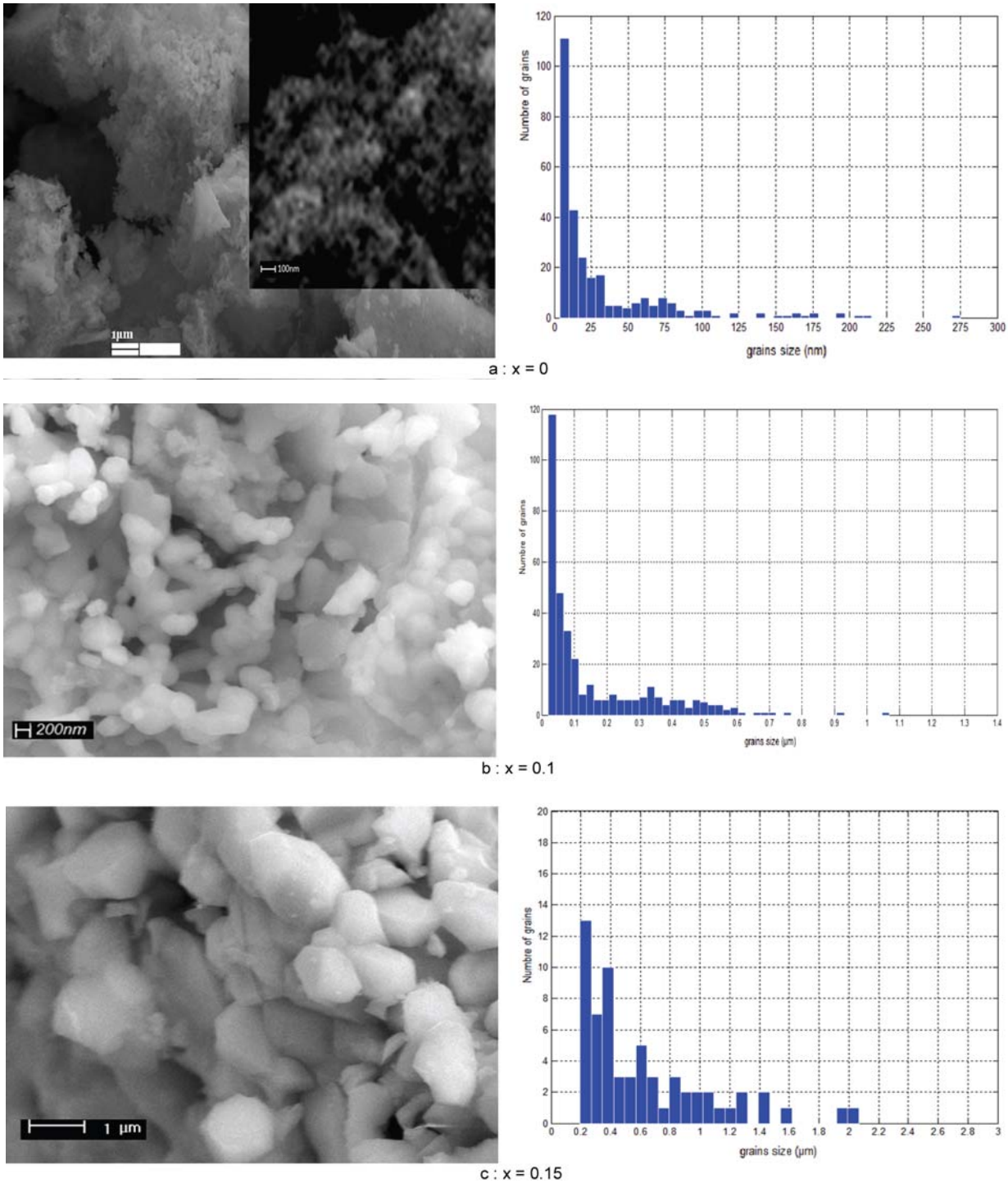

Fig. 3. SEM images and size distribution for $La_{1-x}Sr_xAlO_{3-\delta}$ (x = 0; 0.1; 0.15).

cuit, typical ranges of capacitances of different phenomena are in the order of magnitude of pF/cm^2 for grain interiors (bulk), about 1 nF/cm^2 for grain boundaries, and about 1 µF/cm^2 for external electrode/material interfaces.

Representative impedance spectra at 600 °C (in Nyquist plot using the Zview software) for Sr-substituted series are shown in Figure 4. For all samples, there was just one semicircle at high frequencies indicating that the impedance of the material was predominantly due to the bulk of the grains (intragrain) because of the order of magnitude of the capacitances. The conductivity σ, was calculated from the relationship, σ = L/(R.S), (where L is the thickness and S is the contact area of the electrode). For doped and undoped perovskite, the conductivity in-

creased from $\sigma = 4 \cdot 10^{-8}$ to $\sigma = 3{,}5 \cdot 10^{-6}$ S cm^{-1}at 600 °C for x = 0 to x = 0.1. For x = 0.15, the conductivity decreased to $\sigma = 9 \cdot 10^{-7}$ S cm^{-1} at 600 °C. However, the conductivity for x = 0.15 remained still higher than that of the undoped phase $LaAlO_3$. These changes in conductivity paralleled the changes in the unit cell volume with increasing Sr-content in the composition. Ionic conductivity at higher temperatures is directly related to the creation of oxygen vacancies in these types of doped perovskites. The decrease in conductivity may stem from three plausible facts all of which are linked to solubility of Sr-ions in $LaAlO_3$: i) the appearance of an electrically isolating second phase may decrease the conductivity. This effect could be significant especially if the second phase ($LaSrAl_3O_7$) spreads in the grain boundaries of the conducting matrix phase ($La_{1-x}Sr_xO_{3-\delta}$). In addition to this, ii) the conductivity could further decrease if the amount of oxygen vacancies in the structure of the $La_{1-x}Sr_xO_{3-\delta}$ phase decrease from x = 0.10 to x = 0.15. However, this requires that the case x = 0.10 is a supersaturated state for $La_{1-x}Sr_xO_{3-\delta}$. The moment a second phase precipitates, the amount of Sr in the bulk of $La_{1-x}Sr_xO_{3-\delta}$ decreases to the solubility limit that is in equilibrium with the precipitate ($LaSrAl_3O_7$) phase. The changes in the unit cell volume with increasing Sr-doping support the supersaturation of Sr in $La_{1-x}Sr_xO_{3-\delta}$ bulk with x = 0.10. Te-Yuan Chen et al,[3] reported that the solubility of Sr in the A site of perovskite was limited to 0.20 at a temperature of 1600 °C. The solubility is expected to decrease with decreasing temperature. Therefore it is not unreasonable to expect a solubility limit lower than 10% for Sr at 900 °C. However, this subject requires a further systematic study to report a definitive solubility limit. It should be kept in mind that the formation of a small amount of a second phase was observed for x = 0.10 case. The third explanation for the decrease in conductivity with increasing doubly-charged Sr^{2-} ions could be an association of defects at higher concentration than 10% Sr doping. Such association could also cause slight variations in the unit cell volume. However, it is not possible to predict the direction of changes in the unit cell volume from simple geometric considerations. In the last two cases, the observed second phases at or above x = 0.10 must have been a result of localized disproportionation of Sr ions due to carbonate formation in the precursor. Earlier reports on similar systems have shown that the so-called O_7–phases do disappear at higher temperature anneals.[2]

Figure 5 represents the temperature dependence of the complex impedance spectrum for (a) $La_{0.9}Sr_{0.1}AlO_{3-\delta}$ and (b) $La_{0.85}Sr_{0.15}AlO_{3-\delta}$. Within the range of the current equipment measurable conductivity appears from 500 °C onwards. Between 100 °C and 400 °C, no semi circles were observed. For practical purposes, an ionic conductivity was not present.

The effect of temperature on the conductivity of the specimen was evident from the decrease of impedance as shown in Figure 5; an increase of the temperature of mea-

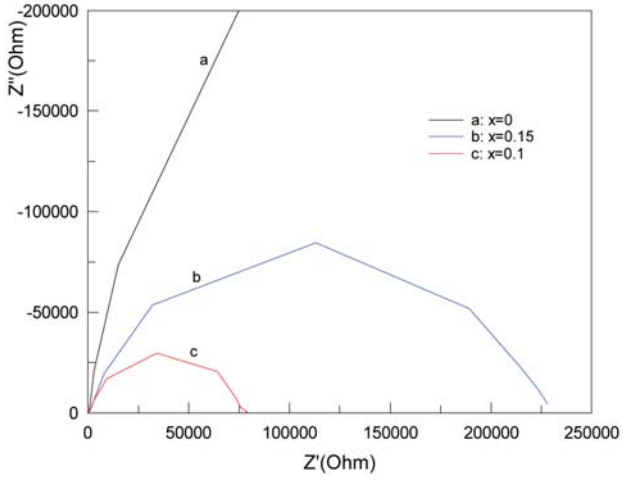

Fig. 4. Impedance spectra at 600 °C for $La_{1-x}Sr_xAlO_{3-\delta}$ (x = 0; 0.1; 0.15).

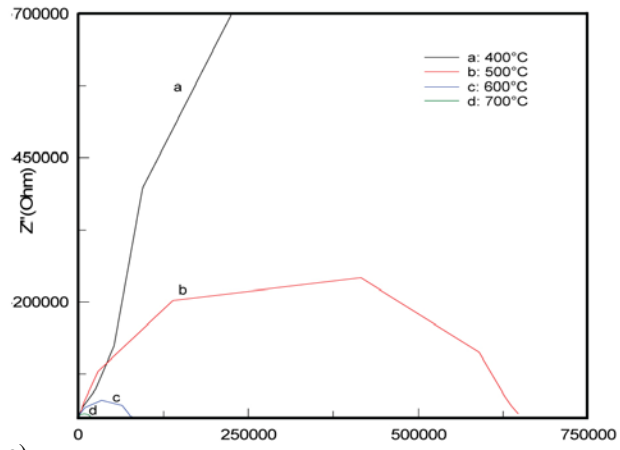

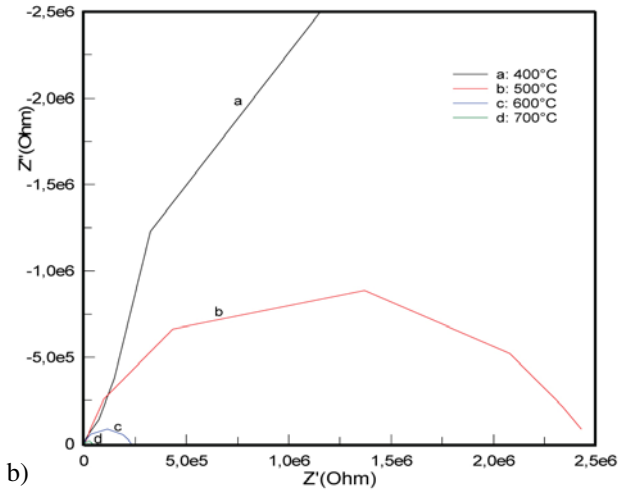

Fig. 5. Impedance spectra for $La_{0.9}Sr_{0.1}AlO_{3-\delta}$ (a) and $La_{0.85}Sr_{0.15}AlO_{3-\delta}$ (b) at different temperatures.

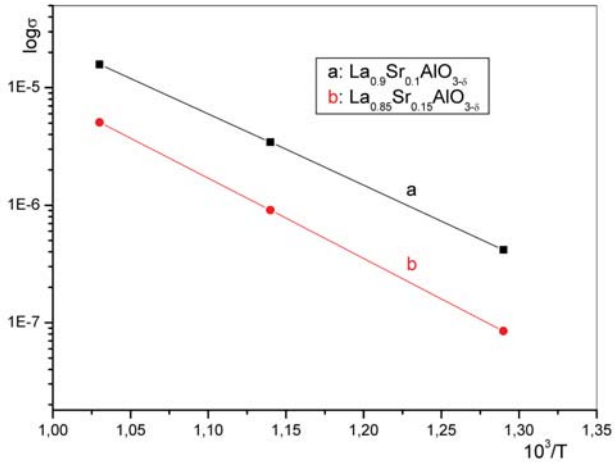

Fig. 6. Arrhenius plot for $La_{0.9}Sr_{0.1}AlO_{3-\delta}$ (a) and $La_{0.85}Sr_{0.15}AlO_{3-\delta}$ (b).

surement leads to an increase in conductivity of the specimens. This can be attributed to the thermally activated mobility of the ions.

Figure 6 depicts the Arrhenius plots of log(σ) versus 1000/T for $La_{0.9}Sr_{0.1}AlO_{3-\delta}$ and $La_{0.85}Sr_{0.15}AlO_{3-\delta}$. The activation energies found for both phases were 1.2 and 1.32 eV, respectively. The increase in the activation energy from x = 0.10 to x = 0.15 paralleled previous XRD results. It should be noted that the two lines are almost parallel and the difference in the activation energy is about 10%. The almost parallel shift in the log conductivity versus 1/T curves indicated that the mechanism of ionic conductivity did not change significantly in the two samples with different Sr-doping amounts. This can be interpreted that the second phase ($LaSrAl_3O_7$) is located as isolated island either within the bulk or at the grain junctions (grain boundaries and multiple grain junctions) but not as a continuous phase at the boundaries. The second phase does not appear to be an effective blocker of the ionic conduction. A confirmation of this statement requires systematic transmission electron microscopy studies of the microstructure.

4. Conclusion

A systematic investigation on structural, morphological and electrical properties of $La_{1-x}Sr_xAlO_{3-\delta}$ (where x = 0, 0.1, 0.15) ceramics were carried out using FTIR, XRD, SEM and impedance spectroscopic techniques. The ceramic powders were prepared by the Pechini process. The gel for $La_{1-x}Sr_xAlO_{3-\delta}$ characterized by FTIR has shown on one side, the chelation between metallic ions and citric acid and on the other side, the polymerization between CA and EG before calcination.

XRD investigations on $La_{1-x}Sr_xAlO_{3-\delta}$ revealed a single perovskite phase for x = 0. Additional diffraction peaks beyond those corresponding to the perovskite phase appeared and can be attributed to the minor secondary phase $LaSrAl_3O_7$ for x = 0.1 and 0.15. The perovskite crystallized in a hexagonal symmetry and the volume cell increased and then decreased with Sr content, showing that the solubility of Sr in $La_{1-x}Sr_xAlO_{3-\delta}$ perovskite is limited to x < 0.15 around 900 °C. The microstructural investigation by SEM revealed that the increase of x in $La_{1-x}Sr_xAlO_{3-\delta}$ increases grain sizes from 33 nm for x = 0 to 600 nm for x = 0.15.

Complex impedance analysis revealed only the bulk contribution, which is temperature and Sr content dependent.

5. References

1. Kai-Yun Yang, Kuan-Zong Fung, Ing-Chi Leu, *Journal of Alloys and Compounds,* **2007**, *438*, 207–216.
2. Ç. Öncel and M. A. Gülgün, in Assessment of Hydrogen Energy for Sustainable Development, Proceedings of the NATO Advanced Research Workshop on Assessment of Hydrogen Energy for Sustainable Development Vol. *VIII*, Edited by J. W. Sheffield and Ç. Sheffield. Energy & Environmental Security, Istanbul, Turkey, **2007**, 147–159.
3. Te-Yuan Chen, Ruo-Ying Pan, Kuan-Zong Fung, *Journal of Physics and Chemistry of Solids,* **2008**, *69*, 540–546.
4. B. Jancar, D. Suvorov, M. Valant, G. Drazic, *J. Eur. Ceram. Soc.,* **2003**, *23*, 1391–1400.
5. I. Zvereva, Y. Smirnov, V. Gusarov, V. Popova, J. Choisnet, *Solid State Sci.,* **2003**, *5*, 343–349.
6. M. Yashima, T. Kato, M. Kakihana, M. A. Gülgün, Y. Matsuo, and M. Yoshimura, *Journal Materials Research,* **1997**, *12(10)*, 2575–2583.
7. M. A. Gulgun, O. O. Popoola, and W. M. Kriven, *J. Am. Ceram. Soc.,* **1994**, *77(2)*, 531–539.
8. Pinyang Fang, Huiqing Fan, Shaojun Qiu, Liajun Liu, Jin Chen, *J Sol-Gel Sci. Technol.,* **2009**, *50*, 290–295.
9. M. A. Gülgün, M. H. Nguyen, and W. M. Kriven, *J. Am. Ceram. Soc.,* **1998**, *82*, 556–560.
10. I. Carazeanu Popovici, V. Ciupina, G. Prodan, M. A. Girtu, *Journal of optoelectronics and Advanced Materials,* **2008**, *10*, 2942–2946.
11. Maggio Pechini, Method of Preparing Lead and Alkaline Earth Titanates and Niobates and Coating Method Using the same to form a capacitor, U. S. Patent No 3 330 697, July 11, **1967**.
12. A. Barabauskas, D. Jasaitis, A. Kareiva, *Vib. Spectrosc.,* **2002**, *28*, 263–275.
13. A. Abreu, S. M. Zanetti, M. A. S Oliveira, G. P. Thim, *J Eur. Ceram. Soc.,* **2005**, *25*, 743–748.
14. J-D Tsay, T-T Fang, T. A. Gubiotti, J. Y. Ying, *J. Mater. Sci.,* 1998, *33*, 3721–3727.
15. M. Kakihana, T. Nagumo, M. Okamoto, H. J. Kakihana, *Phys. Chem.,* **1987**, *91*, 6128–6136.
16. K. Nakamoto, Infrared and Raman spectra of inorganic and coordination compounds, 4th edn. Wiley, New York, **1986**, pp. 231–233.

17. F. Bouremmad, A. Benabbas, N. Bounar, K. Rida, P. Ropa, J-C. Carru, *Functional Materials Letters (FML),* **2009**, *2,* 33–36.
18. N. Sakai, H. Fjellvag, B. Lebech, *Acta Chemica Scandinavica,* **1997**, *51*, 904–909.
19. Rajashree Rajagopal, J. Mona, R. S. Joshee, S. N. Kale, Sivaram Pradhan, A. B. Gaikwad, V. Ravi, *Materials Letters,* **2008**, *62*, 1511–1513.
20. Shuai Li , Bill Bergman, Zhe Zhao, *Journal of the European Ceramic Society,* **2009**, *29*, 1133–1138.
21. B. Schrader, Infrared Raman Spectroscopy: Methods and Application, (Ed.: B. Schrader) VCH, Weinheim, **1995**, pp. 63.
22. H. Bouridah, F. Bouaziz, F. Mansour, R. Mahamdi, P. Temple-Boyer, *Materials Science in Semiconductor Processing,* **2011**, *14*, 261–265.
23. J. Chandradass, Ki Hyeon Kim, *Journal of Alloys and Compounds,* **2009**, *481*, L31– L34.
24. J. X. Zhu, D. F. Zhou, S. R. Guo, J. F. Ye, X. F. Hao, X. Q. Cao, *J. Meng, Journal of Power Sources,* **2007,** *174,* 114– 23.

Povzetek

Delce $La_{1-x}Sr_xAlO_{3-\delta}$ (x = 0, 0,1, 0,15) smo pripravili po Pechinijevem postopku s citronsko kislino in etilenglikolompri temperaturi 900 °C. Prahove smo študirali z vrsto metod fizikalne karakterizacije. Z infrardečo spektroskopijo prekurzorja, segretega pri 200 °C, smo potrdili nastanek metaloorganskega kompleksa in polimerno obliko etilenglikola. Rentgenski spektri vzorcev, segretih pri 900 °C, so potrdili prisotnost enofaznega $LaAlO_3$. Vzorca $La_{0.9}Sr_{0.1}AlO_{3-\delta}$ in $La_{0.85}Sr_{0.15}AlO_{3-\delta}$ sta sestavljena predvsem iz heksagonalne perovskitne faze s sledovi faze $LaSrAl_3O_7$. Ionsko prevodnost v temperaturnem območju od 100 °C do 700 °C v zraku smo študirali z impedančno spektroskopijo.